Frontiers in Chemical Sciences (FCS) 2025, 6(1); 1-13

Calcination Temperature Effects on Ni/ZrO_2 Catalysts for Dry Reforming of Methane

Subhan Azeem[1,2*], Muhammad Rizwan[1], Sadiq Hussain[1]

[1]Department of Chemical Engineering, NFC IET Multan
[2]Department of Food Science and Technology, NFC IET Multan

[*]**Corresponding Author:** msazeem@nfciet.edu.pk

Received:
25th November 2024
Revised:
5th January 2025
Accepted for Publication:
20th January 2025

ABSTRACT

In this study, calcination temperatures (550, 650, and 750 °C) are utilized to analyze the efficiency of Ni-based catalyst for dry reforming of methane (DRM), a potential technique for reduction in greenhouse gases and synthesis of syngas. Ni catalysts were obtained from the impregnation of 10 wt.% Ni onto ZrO_2 prepared in the laboratory. A study of the synthesized catalysts was carried out using characterization techniques such as N_2 physisorption, XRD, FTIR, and SEM. This analysis showed that calcination temperature affects the catalytic activity of the material investigated in the study. For those catalysts showing initially fairly high conversion of methane (more than 50 %), an increase in calcination temperature resulted in a lower conversion of methane. It is believed that Ni nanoparticles sinter at higher temperatures resulting in decreased active surface area of the catalyst which in turn minimizes the number of active sites for the DRM reaction. On the other hand, for the catalysts with lower initial activity below 40 %, the effect of calcination temperature to the catalyst activity was not highly significant. This could be because the Ni particles in these catalysts are larger, or else the metal-support bonds are not so strong that the catalysts cannot resist sintering at high temperatures. From the tested catalysts, NZS-10 has shown the highest performance with the average conversion of CH_4 and CO_2 at 60.5% and 62% respectively, and the lowest deactivation rate of 5%. This superior performance can be attributed to a combination of factors, including high surface area, optimal Ni particle size, strong metal-support interactions, resistance to sintering, and a well-developed porous structure. Fine-tuning certain characteristics of the NZS-10 catalyst can make the catalyst more efficient and have longer stability.

Keywords: DRM, Nickel, ZrO_2, Calcination Temperature, Activity

1. INTRODUCTION

From the current energy mix, fossil fuels are the most abundant providing approximately 85% of the total energy. However, their combustion in the past one and half centuries fuel has resulted in environmental problems mainly global warming brought about by emissions of greenhouse gases. [1-2] There remains a continued use of fossil fuels to cater to global energy needs with the direct consequence of generating greenhouse gases leading to increased air pollution. Unfortunately, the world population continues growing, and when burning non-renewable sources of energy such as fossil fuels, enhances the emission of atmospheric carbon dioxide (CO_2) and other greenhouse gases, which results in climate change. [3-4] Methane (CH_4) is also one of the potent greenhouse gases that has a huge extending impact. [5-7] Thus, dry reforming of methane (DRM) is a promising catalytic technology that can solve environmental problems. It offers a two-fold benefit: improving the environment through decreasing the utilization of greenhouse gases such as CO_2 and CH_4 and redesigning them into significant items. [8-9] The main output of DRM is a hydrogen-

carbon monoxide syngas mixture where H_2 content in the range of 60 to 70% is desirable. This syngas is best when it has an H_2 to CO ratio of between 1 and it is most preferable for the synthesis of liquid hydrocarbons using a Fischer-Tropsch process as pointed. The main DRM reaction is given by Equation (1); other possible side reactions are introduced in Equation (2 - 4).[10] Thus, DRM is the catalytic process that aims at solving environmental problems by using two greenhouse gases, methane (CH_4) and carbon dioxide (CO_2), as raw materials.[11-12] This technology offers a dual advantage: it decreases the amount of CO_2 released to the environment and produces syngas of hydrogen and carbon monoxide gases. Ideally, the H_2/CO ratio of the syngas is close to 1, which is ideal for the production of liquid hydrocarbons through the Fischer-Tropsch synthesis.[8] The main DRM reaction is depicted by the following equation: However, several side reactions can take place, including; disproportionation, methane cracking, and the reverse water-gas shift reaction which is important in the formation of H_2O.[13] Based on the literature, DRM is a promising research area due to the potential for greenhouse gas reductions.[13-14] But it is an endothermic process and it requires high temperatures to execute this process perfectly. This results in the fast deactivation of the catalyst that limits its use in industries. High temperatures also affect the rate of methane decomposition and coke formation.

Conventional metal supports, with the use of Ni and other transition metals, are widely incorporated in DRM. Although noble metals are outstanding in activity and stability, they usually cost much and are scarce on Earth. Thus, the performance of supported catalysts depends on the nature of the support material and the dispersion of the active metal sites over the support material.[15-17] The practical method for minimizing the formation of carbon and also in increasing the lifetime of the catalyst is by adding various supports to the nickel-based catalysts. Dry reforming reactions are carried out mainly using supported metal catalysts in which the metal particles are dispersed on a high surface area material known as the support.[18-19] The materials that are commonly used for support are alumina (Al_2O_3), silica (SiO_2), and zirconia (ZrO_2) support.[20-22] It is here that one can single out one of the principal factors affecting the performance of the catalyst – the choice of the support material. For instance, initial supports such as ZrO_2 can improve CO_2 adsorption and decomposition conclusion that stirs a good metal-support relationship that may help decrease carbon build-up.[1, 13, 23] Also, the support has the characteristics of oxygen storage, which might be helpful in DRM. For the ideal scenario, the support should offer a stable and large open surface area for uniform distribution of the active metal phase to hinder it from sintering. It can also help in the reaction mechanism since it may help in the activation of CO_2.[24] Among the supports, Zirconia (ZrO2) is preferred provided its availability and footing on different crystallographic tolerant styles such as cubic, monoclinic, and tetragonal.[25-26]

Thus, the phase that is attained by ZrO_2 depends greatly on characteristics like temperature, dopants, the method of preparation, oxygen vacancies, and crystallite size.[27] Calcination pretreatment plays an important role in catalyst preparation because it alters the nature of the support material.[28] Studies of the effect of calcination temperature on different catalysts are described in the literature.[29-32] Low calcination temperatures may cause only partial decomposition of the metal precursor: therefore, the catalyst contains a lower concentration of active sites. On the other hand, very high temperatures can lead to the sintering of the active metal particles thus decreasing the surface area and upholding the supporter morphology. Many authors have researched the effect of calcination on the activity of the catalyst in various systems of reactions. The Fischer-Tropsch synthesis studies have illustrated that increasing the temperature in air to cause calcination increases the selectivity of some of the catalysts in favor of certain products [33]. Likewise,

Sun et al. reported that calcination temperature influenced the activity of the catalysts for dry reforming through the oxidation state of the active metal and types of functional groups on the support.[33]

The objectives of the present research were to establish the synergistic impact of zirconia support and calcination temperature for DRM catalysts. In this study, 10% nickel supported on ZrO_2 prepared through the impregnation method and measured their activity in DRM. The calcination tests were carried out keeping in view the effect of this pre-treatment step on the general applicability of 10% Ni/ZrO_2 catalysts. Based on the aforementioned aspects, it was anticipated that calcination would induce significant alterations to the specific properties, e.g., surface area, and metal dispersion of the catalysts, which in turn may have implications for their performance in DRM. The catalysts in this study were subjected to calcination at three specific temperatures: 550, 650, and 750 °C, respectively. This range was selected to study the effect of calcination treatment on the catalyst characteristics and surface features about the possible consequences of the high or low temperature.

2. MATERIALS AND METHODS

2.1 Synthesis of Material

5.0 g (EO)20(PO)70(EO)20 triblock copolymer (Pluronic P123 from BASF, Co.) was used to synthesize the mesoporous zirconia support, which was then dissolved in 50.0 mL of anhydrous ethanol while being constantly stirred at room temperature for 4 hours. In a separate step, 80 mL of zirconium (IV) n-butoxide (an 80weight percent solution in 1-butanol) was dissolved in a mixture of 20 mL of 68-70 wt% nitric acid and 50.0 mL of anhydrous ethanol. The two solutions were then combined and stirred at room temperature for 4 hours. The mixture was then placed in an oven and kept at 100 °C for 24 hours to evaporate the solvent, and the solid was then calcined at 500 °C for 5 hours. The wet impregnation method was used to incorporate nickel into the zirconia support. After dissolving the desired amount of nickel nitrate hexahydrate ($Ni(NO_3)_2 \cdot 6H_2O$) in distilled water, the calculated amount of zirconia support was added to the nickel nitrate solution and stirred continuously for three hours at room temperature (26 ± 2 °C). During the first six hours of the drying process at room temperature, the slurry was manually stirred every hour to prevent agglomeration. The dried catalyst was then crushed, sieved, and calcined at 550, 650, and 750°C for five hours at a heating rate of 5 °C/min. The final catalysts were labeled NZS-10 and NZR-10, where the number indicates the nickel loading in weight percent.

2.2 Catalyst Characterization

High-resolution X-ray diffraction (XRD) analysis was performed on a Bruker D2-Phaser diffractometer. Cu Kα radiation was used as the X-ray source, and data was collected over a 2θ range of 10-80° with an operating voltage of 40 kV and a current of 200 mA. Before analysis, samples were degassed under a vacuum at 300°C for three hours. This allowed for the determination of the textural properties of the synthesized catalysts, such as specific surface area, pore size, and pore volume, using N_2 adsorption-desorption analysis on a Nova 2200e Quanta chrome surface area analyzer and N_2 adsorption-desorption analysis.

The catalysts' surface chemistry was described using Fourier Transform Infrared Spectroscopy (FTIR). A Shimadzu 8400 FTIR spectrometer was used to record FTIR spectra. For analysis, KBr pellets were made at room temperature. Scanning electron microscopy (SEM) was used to analyze the catalysts' shape and particle size distribution. Utilizing an FEI Titan 200 Scanning Electron Microscope, high-resolution pictures were acquired.

2.3 Catalysts Performance

The catalytic performance of the synthesized catalysts was evaluated in a fixed-bed flow reactor. Before the reaction, catalysts were pre-reduced in situ at 550 °C for 120 minutes under a hydrogen flow rate of 50 ml/min. The dry reforming of methane (DRM) reaction was conducted at 1 bar pressure using a 50:50 molar ratio of methane to carbon dioxide, with both gases having a purity of 99.995%. Reaction parameters, such as temperature, pressure, and gas hourly space velocity (GHSV), were maintained constant for all catalyst systems. Reaction temperature was monitored using a thermocouple placed within the reactor bed. Product analysis was performed using an online gas chromatograph equipped with a Thermal Conductivity Detector (TCD) and helium as the carrier gas. Methane and carbon dioxide conversions were calculated using the following equations:

$$X_{CH4}\ (\%) = 100 \times F_{CH4in} - F_{CH4out} / F_{CH4in} \quad (1)$$

$$X_{CO2}\ (\%) = 100 \times F_{CO2in} - F_{CO2\ out} / F_{CO2in} \quad (2)$$

The deactivation factor (DFA) of each catalyst was determined using the following equation

$$DFA = 100 \times X_{iCH4} - X_{fCH4} / Xi_{CH4} \quad (3)$$

where Xi_{CH4} represents the initial methane conversion and X_{fCH4} represents the final methane conversion.

3. RESULTS AND DISCUSSIONS

3.1 N_2-Adsorption-Desorption

The N_2 physisorption isotherms of the catalysts are shown in Figure 1. The type IV isotherms of the material contain an H1 hysteresis loop typical for the relative pressures higher than P/P0. This characteristic corresponds to the IUPAC classification which indicates the predominantly mesopores with an ordered structure. The plots show that the N_2 adsorption rises sharply in the vicinity of P/Po =0. 75. This shows that the process of capillary condensation that takes place in the mesopores or macropores is interconnected. This behavior is manifested when the critical temperature of the adsorbate is greater than the adsorption temperature. Remarkably, the mesoporous supports can help in the formation of the active carbon that easily undergoes the gasification process. The nitrogen physisorption data of NZS-10 and NZR-10 catalysts were in the same fashion as shown in Figure 1(a, b, and c). By increasing the calcination temperature, the amount of N_2 adsorption is reduced, which correlates with the surface area results obtained. Such a reduction in the surface area with increasing calcination temperatures is well understood for ZrO_2-based systems. This believed that it sintered the ZrO_2 crystallites in which particles with lower particle size coalesce to the formation of larger and densely packed domains. The previous authors' study by Chan et al. concerned themselves with the influence [34-35] of calcination temperature when preparing ZrO_2 and also recorded the above results of our ZrO_2-supported Ni catalysts when investigating calcination temperature and also noticed that the phase transformation contributed little to the reduction in surface area at higher temperatures [34]. Additional information about the pore size distribution of catalysts calcined at different temperatures is given in Figure 2 (a, b, and c). These values supports that the pores are mesoporous and the porosity increases with calcination temperature. The catalysts showed an increase in pore volume coupled

with an increase in pore size especially at lower pore size values. The textural properties of the catalysts are shown in table 1.

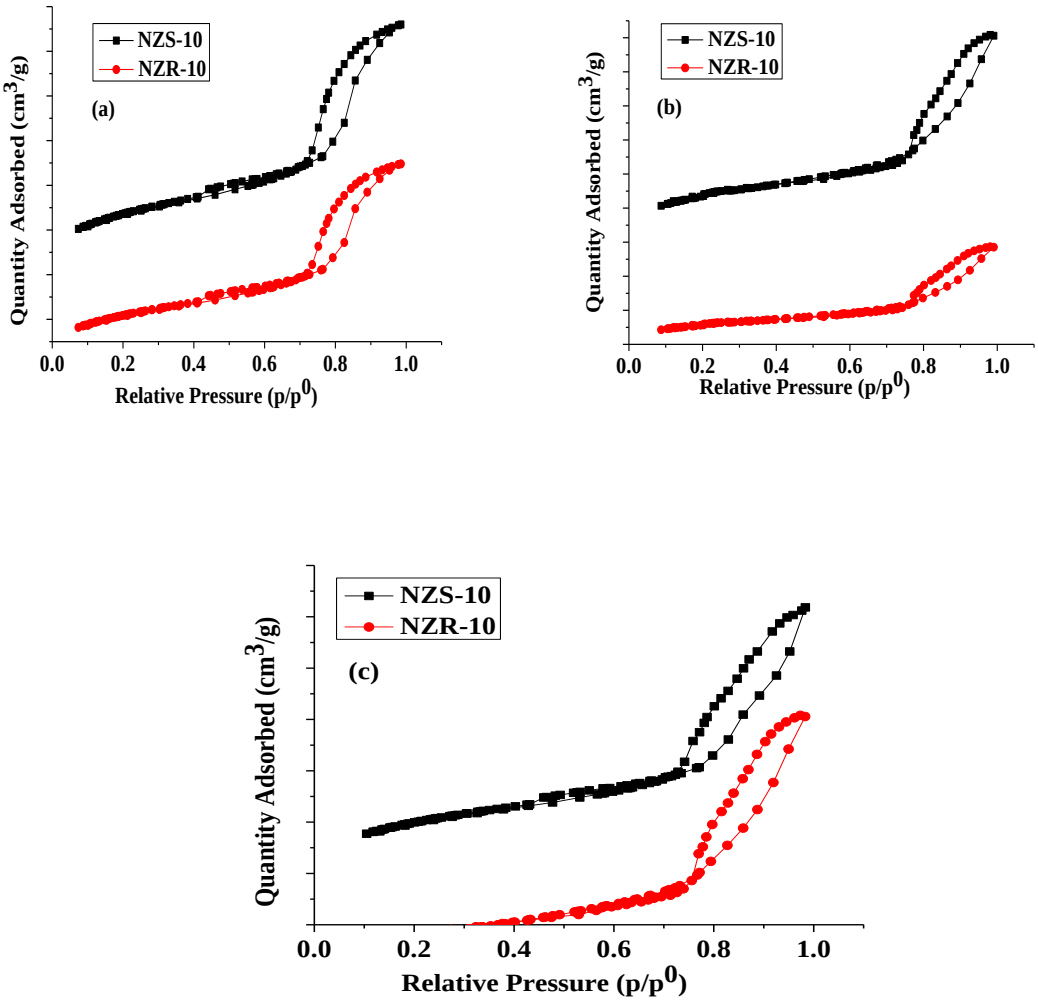

Figure 1. N_2 Physisorption isotherms of the Catalysts Calcined at Temperature (a=550 ^{0}C b= 650 ^{0}C and c= 750 ^{0}C)

Table 1. Textural Properties of the Calcined Catalysts

Catalyst	Calcination Temperature (^{0}C)	Surface area (s_g) cm^2/g	BJH (d_p) nm	BJH (V_p) cm^3/g
NZR-10	550	38.6	16.7	0.22
	650	21.1	27.8	0.14
	750	20.7	27.3	0.13
NZS-10	550	27.5	35.5	0.19
	650	14.7	37.1	0.12

750	14.3	36.8	0.11

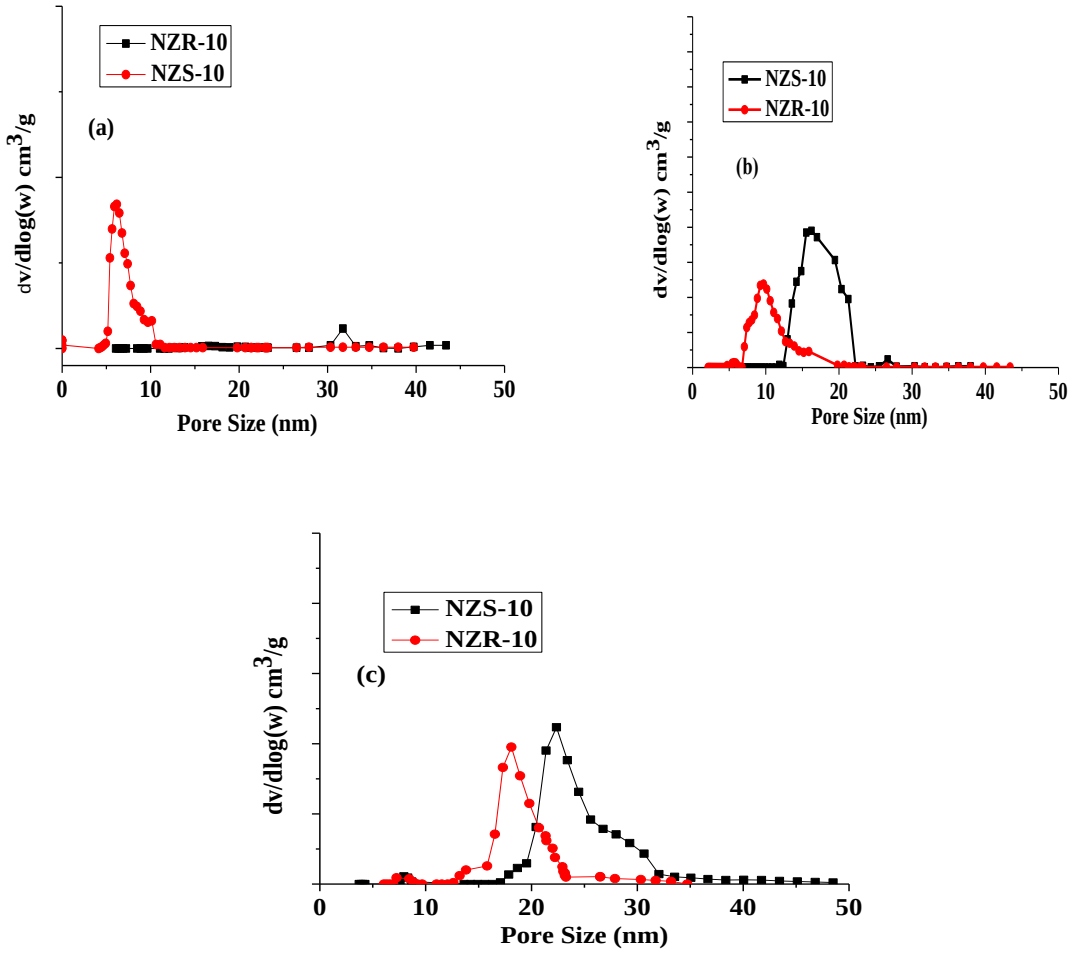

Figure 2. Pore Size Distribution of the Catalysts Calcined at Temperature (a=550 ^{0}C b= 650 ^{0}C and c= 750 ^{0}C)

3.2 FTIR Analysis

Fourier-transform infrared (FTIR) spectroscopy was employed to investigate the surface properties and identify functional groups of the calcined 10% Ni/ZrO_2 catalysts in Figure 3. The specific bands at the 500-585 cm^{-1} range corresponding to the Zr-O vibrations of the zirconia support are still discernible. In addition, the band in the range of 700-760 cm^{-1}, characterized a tetragonal zirconia phase and contributed to the understanding of the structural properties of the support material. Specifically, the FTIR spectra of the Ni/ZrO_2 catalysts were characterized by one or two additional bands in the range of 500–585 cm $^{-1}$. These bands are suggested to result from the formation of Ni-O-Zr bonds at the interface between the nickel nanoparticles and the zirconia support [34]. The existence of these bands indicates high metal-support interaction that is critical in most applications for boosted catalytic performance and durability. These FTIR results are useful in understanding the surface features of the catalysts, the effects of support characteristics, and the nature of metal-support interaction for the performance of the catalysts. It has been demonstrated that metal-support interactions can indeed improve the catalytic performance due to electron exchange

between the metal and the support, activation of the reactants, and resistance of the active sites against sintering.

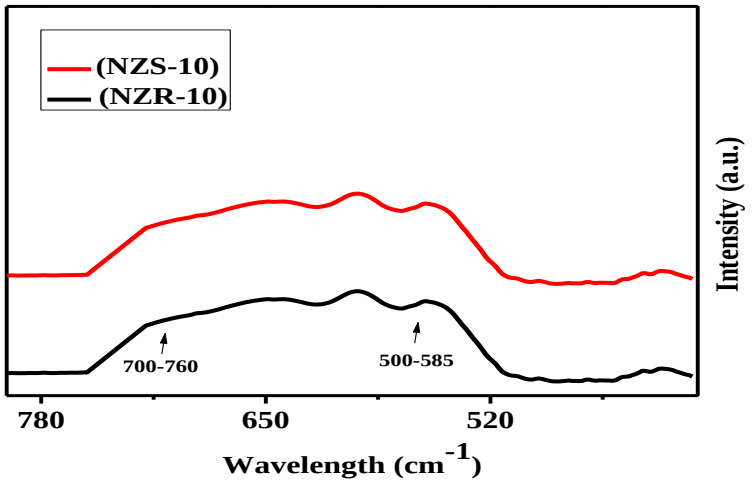

Figure 3. FTIR Spectra of the Catalysts supported on zirconia

3.3 XRD Analysis

XRD analysis revealed the presence of crystalline phases corresponding to both Ni and ZrO_2 is shown in Figure 4. Characteristic peaks of Ni were observed at 37.7° and 42.1° 2θ. The zirconia support exhibited a mixed phase, with peaks at 18.4°, 24.5°, 27.6°, 63.0°, 69.5°, and 75.6° attributable to the monoclinic phase (JCPDS file No. 81-1314) and peaks at 29.6°, 34.6°, 50.1°, and 59.8° corresponding to the tetragonal phase of zirconia.[36] Interestingly, in the NZS-10 catalyst small peaks attributed to NiO were observed in the XRD patterns, suggesting the presence of larger NiO crystallites. In contrast, the characteristic peaks of NiO were less prominent or absent in the NZR-10 catalyst, indicating a more uniform dispersion of nickel species within the zirconia support. This suggests that calcination temperature may have influenced the interaction between nickel and the zirconia support, potentially leading to smaller and more dispersed Ni particles. Such conditions of calcination could affect the phase composition of zirconia which may in turn influence its surface features and interfacial interaction with Ni nanoparticles. The strength and nature of the metal-support interaction that is central to the determination of catalytic activity can be affected by the calcination process. Metal-support interactions with stronger binding can improve the dispersion of Ni nanoparticles, the electron transfer conductivity, and the stability of the active sites against sintering. The calcination temperature may also affect the probability of the formation of coke on the surface of the catalyst on the active sites.

3.4 SEM Analysis

To further investigate the surface morphology of the best-performing catalyst, NZS-10, scanning electron microscopy (SEM) analysis was performed. Figure 5 a, b), depict the morphology of the fresh catalyst, revealing a well-dispersed distribution of small nickel nanoparticles on the surface of the zirconia support. This uniform distribution of active sites is crucial for efficient catalytic activity in DRM, as it maximizes the contact between the reactant molecules and the active metal sites.

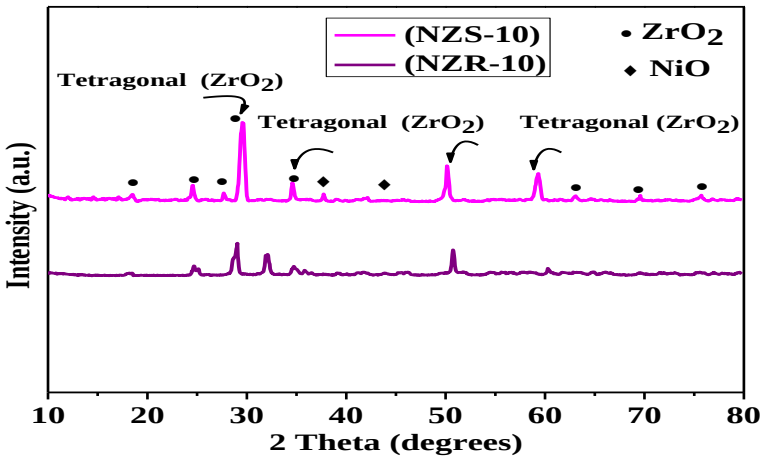

Figure 4. FTIR Spectra of the Catalysts supported on zirconia

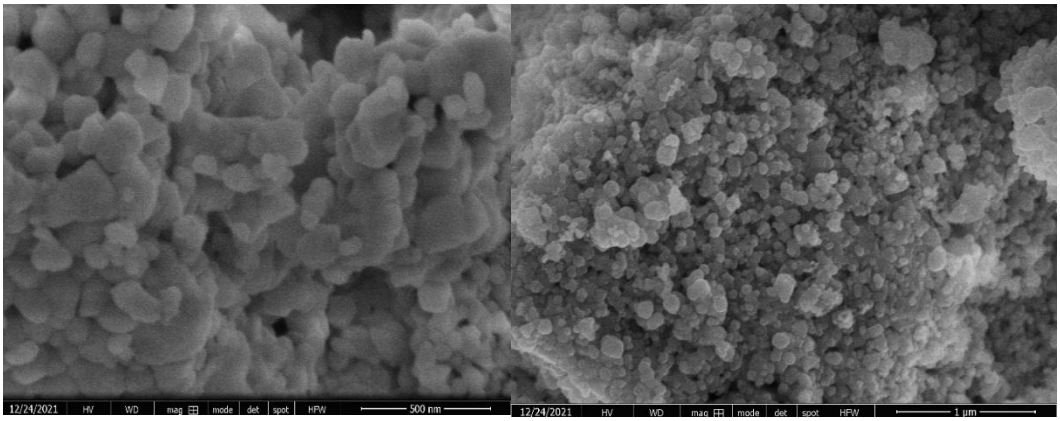

Figure 5 (a, b). SEM micrographs of the Catalyst

3.5 Catalysts Activity Results

The catalytic activity of Ni/ZrO_2 catalysts was evaluated for dry reforming of methane (DRM). It was also noticed that with time there is a slow reduction in the conversion of both methane and carbon dioxide during the reaction due to catalyst deactivation. Notably, a higher CO_2 conversion compared to CH_4 conversion was observed in several cases, which can be attributed to the occurrence of the reverse water-gas shift reaction. The effect of calcination temperature on catalytic activity exhibited a distinct trend. For catalysts with initially high methane conversion (above 50%), increasing the calcination temperature generally led to a decrease in activity. This trend suggests that higher calcination temperatures may lead to sintering of Ni nanoparticles, resulting in a decrease in active surface area and a decline in catalytic activity.[27, 35]

On the other hand, for the samples with less initial activity below 40% as shown in Figure 6 (a, b, and c) and 7 (a, b, and c), It was observed that the variation of the calcination temperature did not have greatly affect its activity. This may be attributed to several factors, including: The low initial activity of some of the catalysts may already possess faults like low metal dispersion or weak metal support interaction which may not be further accentuated by raising the calcination temperature. Raising calcination temperature may reduce some extent of sintering but may also have beneficiated other properties such as metal-support

interaction or reducibility. Among the tested samples, the NZS-10 catalyst calcined yielded the best result with a conversion of CH_4 and CO_2 average at 60.5% and 62% respectively, and the overall deactivation factor of 5% signifying relatively high stability of the catalyst under reaction conditions as shown in Table 2. A lower deactivation factor thus reflects more catalyst stability and a longer catalyst lifetime therein implies that it will perform for a longer period without degrading in activity. For instance, an NZS-10 catalyst with a low deactivation factor translates to longer activity and, thus, higher potential for its use in industries. This implies that for this particular catalyst, there is a desirable compromise between high surface area, good interaction between the metal and the support, and sintering resistance [37]. The changes in the catalytic activity that have been observed with increasing calcination temperature are likely due to several reasons: calcination leads to a change in the morphology of the ZrO_2 support, including the surface area and pore structure and the interaction of the Ni nanoparticles. By varying calcination conditions, the strength and nature of the interaction between the metal and the support can be altered—a factor that determines the catalytic performance and robustness of the final catalyst. The temperature at which calcination occurs can affect the tendency of coke deposition on this catalyst surface since this inextricably affects catalytic activity. This is due to the complexity of the analyzed materials and the need for additional, in-situ characterization techniques to determine the exact processes that stand behind the observed trends in catalytic ability dependence on calcination temperature.

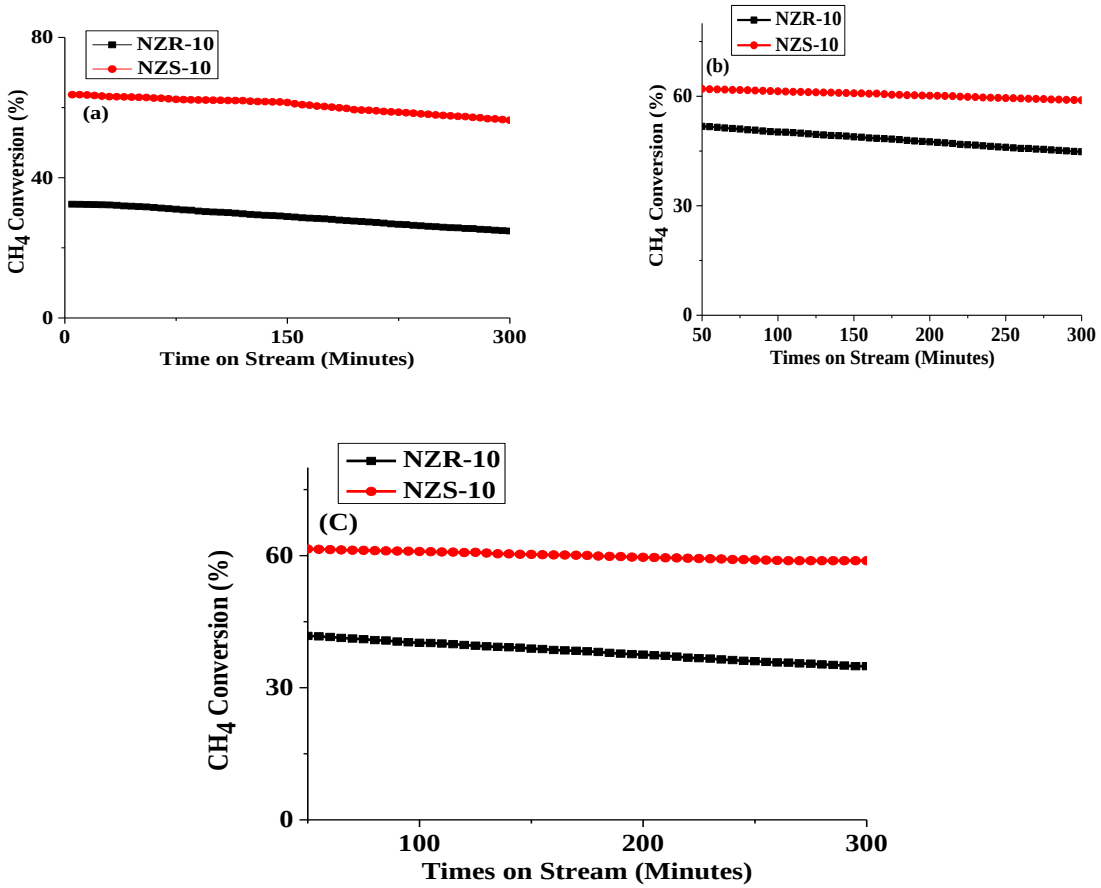

Figure 6. Performance evaluation of the catalysts in the terms of CH_4 Conversion (%) Calcined at different temperature (a) 550 ^{0}C (b) 650 ^{0}C (C) 750 ^{0}C

Table 2. Catalysts Performance at different Calcination Temperature (^{0}C)

Catalyst	Calcination Temperature (^{0}C)	CH_4 Conversion (%)		CO_2 Conversion (%)		DFA (%)
		Initial	Final	Initial	Final	
NZS-10	550	32.45	24.79	36.39	32.98	24.5
	650	52.45	44.8	54.92	49.91	18.8
	750	42.67	34.9	42.98	35.03	15.3
NZR-10	550	63.68	58.39	64.52	59.91	8.3
	650	62.39	58.91	65.87	51.39	5.6
	750	61.99	58.83	64.43	59.63	5.3

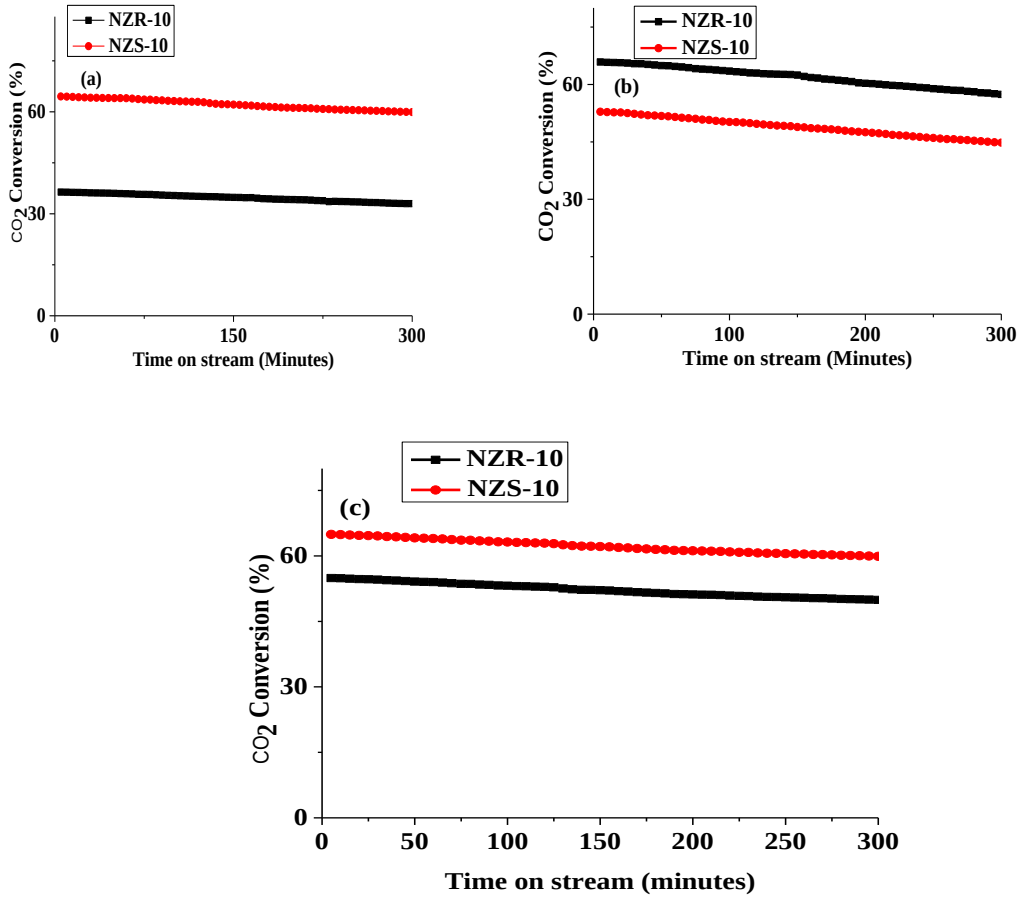

Figure 7. Performance evaluation of the catalysts in the terms of CO_2 Conversion (%) Calcined at different temperature (a) 550 ^{0}C (b) 650 ^{0}C (C) 750 ^{0}C

4. CONCLUSION

The purpose of this work was to determine the effect of the calcination temperature of 10% Ni/ZrO_2 catalyst on the catalytic activity during dry reforming of methane (DRM). Ni catalysts were obtained by impregnating nickel onto synthesized in-house zirconia supports, calcined at different temperatures of 550

°C, 650 ºC, and 750 ºC. Characterization techniques, including N_2-physisorption, XRD, FTIR, and SEM, were employed to elucidate the structure-property relationships of the synthesized catalysts. The NZS-10 catalyst exhibited superior performance with higher surface area and smaller particle size, indicating a strong correlation between structural properties and catalytic activity. XRD analysis revealed the presence of both monoclinic and tetragonal phases of zirconia in the fresh stabilized catalysts. SEM analysis of the best-performing catalyst NZS-10 showed well-dispersed small nickel particles on the support surface, suggesting optimal metal-support interaction.

The effect of calcination temperature on catalytic activity varied significantly. Catalysts with initially high methane conversion exhibited a decrease in activity with increasing calcination temperature, likely due to sintering of Ni nanoparticles, which reduces the available active surface area. Conversely, for catalysts with lower initial activity, the impact of calcination temperature was less pronounced, suggesting that other factors, such as pre-existing limitations in metal dispersion or weaker metal-support interactions, might be more dominant. The NZS-10 catalyst demonstrated the highest performance with average CH_4 and CO_2 conversions of 60.5% and 62%, respectively, and a low deactivation factor of 5%. This suggests an optimal balance between high surface area, strong metal-support interaction, and resistance to sintering in this particular catalyst. These findings highlight the crucial role of calcination temperature in optimizing the performance of Ni/ZrO_2 catalysts for DRM. Further investigations are necessary to fully understand the interplay between calcination temperature, support properties, and metal particle characteristics in determining the catalytic activity and stability of these materials.

REFERENCES

1. Al-Fatesh, A. S.; Patel, N.; Srivastava, V. K.; Osman, A. I.; Rooney, D. W.; Fakeeha, A. H.; Abasaeed, A. E.; Alotibi, M. F.; Kumar, R., Iron-promoted zirconia-alumina supported Ni catalyst for highly efficient and cost-effective hydrogen production via dry reforming of methane. *journal of environmental sciences* **2025,** *148*, 274-282.
2. Teh, L.; Setiabudi, H.; Timmiati, S.; Aziz, M.; Annuar, N.; Ruslan, N., Recent progress in ceria-based catalysts for the dry reforming of methane: A review. *Chemical Engineering Science* **2021,** *242*, 116606.
3. Karmaker, A. K.; Rahman, M. M.; Hossain, M. A.; Ahmed, M. R., Exploration and corrective measures of greenhouse gas emission from fossil fuel power stations for Bangladesh. *Journal of Cleaner Production* **2020,** *244*, 118645.
4. Dang, C.; Yu, H., Bifunctional catalysts for the coupling processes of CO 2 capture and conversion: a minireview. *Reaction Chemistry & Engineering* **2025**.
5. Shahzad, U.; Fareed, Z.; Shahzad, F.; Shahzad, K., Investigating the nexus between economic complexity, energy consumption and ecological footprint for the United States: New insights from quantile methods. *Journal of Cleaner Production* **2021,** *279*, 123806.
6. Balopi, B.; Gorimbo, J.; Moyo, M., Reforming as a green technology for the utilization of biogas. In *Innovations in the Global Biogas industry*, Elsevier: 2025; pp 181-209.
7. Liu, H.; Tang, Y.; Ma, X.; Tang, J.; Deng, J.; Yue, W., Calcium looping-enhanced biomass gasification for methanol production: Integrating methane dry reforming and carbon utilization. *Separation and Purification Technology* **2025,** *354*, 129377.
8. SUN, K.; JIANG, J.; LIU, Z.; GENG, S.; LIU, Z.; YANG, J.; LI, S., Research progress on metal-support interactions over Ni-based catalysts for CH 4-CO 2 reforming reaction. *Journal of Fuel Chemistry and Technology* **2025**.
9. Yousefi, S.; Tavakolian, M.; Rahimpour, M. R., Bio-templated Ni/MgO-Al2O3 as an efficient catalyst toward methane dry reforming. *Inorganic Chemistry Communications* **2025,** *171*, 113557.

10. Ibrahim, A. A.; Fakeeha, A. H.; Abasaeed, A. E.; Al-Fatesh, A. S., Dry Reforming of Methane Using Ni Catalyst Supported on ZrO2: The Effect of Different Sources of Zirconia. *Catalysts* **2021,** *11* (7), 827.
11. bin Jumah, A.; Kaydouh, M.-N.; Al-Fatesh, A. S.; Bayazed, M. O.; Fakeeha, A. H.; Ibrahim, A. A.; Abasaeed, A. E.; Chaudhary, K. J.; El Hassan, N., Cerium-induced modification of acid-base sites in Ni-zeolite catalysts for improved dry reforming of methane. *Journal of the Energy Institute* **2025,** *118*, 101901.
12. Song, J.; Fan, Y.; Wang, F.; Shi, X.; Li, C.; Du, J.; Yi, H., Thermodynamic analysis of a novel compressed carbon dioxide energy storage coupled dry methane reforming system with integrated carbon capture. *Applied Energy* **2025,** *377*, 124769.
13. Khatun, R.; Pal, R. S.; Bhati, K.; Kothari, A. C.; Singh, S.; Siddiqui, N.; Rana, S.; Bal, R., Ni/Ce 0.8 Zr 0.2 O 2-x Solid Solution Catalyst: A Pathway to Coke-Resistant CO 2 Reforming of Methane. *RSC Sustainability* **2025**.
14. Abasaeed, A.; Kasim, S.; Khan, W.; Sofiu, M.; Ibrahim, A.; Fakeeha, A.; Al-Fatesh, A., Hydrogen yield from CO2 reforming of methane: impact of La2O3 doping on supported Ni catalysts. *Energies* **2021,** *14* (9), 2412.
15. Patel, R.; Al-Fatesh, A. S.; Fakeeha, A. H.; Arafat, Y.; Kasim, S. O.; Ibrahim, A. A.; Al-Zahrani, S. A.; Abasaeed, A. E.; Srivastava, V. K.; Kumar, R., Impact of ceria over WO3–ZrO2 supported Ni catalyst towards hydrogen production through dry reforming of methane. *International Journal of Hydrogen Energy* **2021,** *46* (49), 25015-25028.
16. Al-Fatesh, A. S.; Fakeeha, A. H.; Ibrahim, A. A.; Abasaeed, A. E., Ni supported on La2O3+ ZrO2 for dry reforming of methane: the impact of surface adsorbed oxygen species. *International Journal of Hydrogen Energy* **2021,** *46* (5), 3780-3788.
17. Ibrahim, A. A.; Al-Fatesh, A. S.; Khan, W. U.; Kasim, S. O.; Abasaeed, A. E.; Fakeeha, A. H.; Bonura, G.; Frusteri, F., Enhanced coke suppression by using phosphate-zirconia supported nickel catalysts under dry methane reforming conditions. *International Journal of Hydrogen Energy* **2019,** *44* (51), 27784-27794.
18. Ma, X.; Yang, W.-W.; Zhang, J.-R.; Tang, X.-Y., Structural evolution of Ni-Ce bimetallic alloy on Al2O3 support in methane dry reforming: Achieving sustainability and high-efficiency reaction through cerium modulation strategy. *Fuel* **2025,** *384*, 134084.
19. Lian, Z.; Xiao, Z.; Zhang, J.; Zhang, X.; Wang, L.; Zou, J.-J.; Li, G., Controllable adjustment of nickel accessibility on CeO2 by hard template for efficient hydrogen production via steam reforming of methane. *International Journal of Hydrogen Energy* **2025,** *99*, 716-728.
20. Ramteke, S. M.; Meshram, S. A.; Chelladurai, H.; Choudhary, A. K., Thermochemical hydrogen production methods: A review. *Hydrogen Energy* **2025**, 130-147.
21. Shukla, A. K.; Gautam, R.; Chaudhary, S.; Srivastava, A. K.; Kumar, A.; Singh, S.; Maurya, P. K., Hydrogen energy: Addressing challenges and exploring future prospects. In *Hydrogen Energy*, CRC Press: 2025; pp 34-45.
22. Memarian, Z.; Meshkani, F., CO2 reforming of glycerol on Ni/Al2O3 catalyst: Influence of doping of alkaline earth metals (Mg, Ca, Sr, and Ba) to support. *Biomass and Bioenergy* **2025,** *193*, 107578.
23. Saldaña, J.; Yurukcu, M.; Boppana, N.; Arbabi, S.; Henry, J.; Ziyanak, S., 10 Hydrogen Energy and Technologies. *Energy Transition in the Oil and Gas Industry* **2025,** *47*, 356.
24. Aramouni, N. A. K.; Zeaiter, J.; Kwapinski, W.; Leahy, J. J.; Ahmad, M. N., Molybdenum and nickel-molybdenum nitride catalysts supported on MgO-Al2O3 for the dry reforming of methane. *Journal of CO2 Utilization* **2021,** *44*, 101411.
25. McCullough, J. t.; Trueblood, K., The crystal structure of baddeleyite (monoclinic ZrO2). *Acta Crystallographica* **1959,** *12* (7), 507-511.
26. Chen, A.; Zhou, Y.; Miao, S.; Li, Y.; Shen, W., Assembly of monoclinic ZrO 2 nanorods: formation mechanism and crystal phase control. *CrystEngComm* **2016,** *18* (4), 580-587.

27. Zhang, M.; Zhang, J.; Zhou, Z.; Chen, S.; Zhang, T.; Song, F.; Zhang, Q.; Tsubaki, N.; Tan, Y.; Han, Y., Effects of the surface adsorbed oxygen species tuned by rare-earth metal doping on dry reforming of methane over Ni/ZrO2 catalyst. *Applied Catalysis B: Environmental* **2020,** *264*, 118522.
28. Yang, E.-h.; Moon, D. J., CO 2 Reforming of Methane over Ni 0/La 2 O 3 Catalyst Without Reduction Step: Effect of Calcination Atmosphere. *Topics in Catalysis* **2017,** *60*, 697-705.
29. Zhang, M.; Zhang, J.; Zhou, Z.; Zhang, Q.; Tan, Y.; Han, Y., Effects of calcination atmosphere on the performance of the co-precipitated Ni/ZrO2 catalyst in dry reforming of methane. *The Canadian Journal of Chemical Engineering* **2022,** *100*, S172-S183.
30. Ji, B.; Li, Q.; Huang, Q.; Zhang, W., Enhanced leaching recovery of rare earth elements from a phosphatic waste clay through calcination pretreatment. *Journal of Cleaner Production* **2021,** *319*, 128654.
31. Aramouni, N. A. K.; Zeaiter, J.; Kwapinski, W.; Leahy, J. J.; Ahmad, M. N., Trimetallic Ni-Co-Ru catalyst for the dry reforming of methane: Effect of the Ni/Co ratio and the calcination temperature. *Fuel* **2021,** *300*, 120950.
32. Fertal, D. R.; Monai, M.; Proano, L.; Bukhovko, M. P.; Park, J.; Ding, Y.; Weckhuysen, B. M.; Banerjee, A. C., Calcination temperature effects on Pd/alumina catalysts: Particle size, surface species and activity in methane combustion. *Catalysis Today* **2021,** *382*, 120-129.
33. Sun, Y.; Zhang, G.; Xu, Y.; Zhang, R., Catalytic performance of dioxide reforming of methane over Co/AC-N catalysts: Effect of nitrogen doping content and calcination temperature. *International Journal of Hydrogen Energy* **2019,** *44* (31), 16424-16435.
34. Chan, K.; Chuah, G.; Jaenicke, S., Preparation of stable, high surface area zirconia. *Journal of materials science letters* **1994,** *13*, 1579-1581.
35. Chuah, G.; Jaenicke, S.; Cheong, S. A.; Chan, K., The influence of preparation conditions on the surface area of zirconia. *Applied Catalysis A: General* **1996,** *145* (1-2), 267-284.
36. Sun, J.; Yamaguchi, D.; Tang, L.; Periasamy, S.; Ma, H.; Hart, J. N.; Chiang, K., Enhancement of oxygen exchanging capability by loading a small amount of ruthenium over ceria-zirconia on dry reforming of methane. *Advanced Powder Technology* **2022,** *33* (2), 103407.
37. Al-Fatesh, A. S.; Arafat, Y.; Ibrahim, A. A.; Kasim, S. O.; Alharthi, A.; Fakeeha, A. H.; Abasaeed, A. E.; Bonura, G.; Frusteri, F., Catalytic behaviour of Ce-doped Ni systems supported on stabilized zirconia under dry reforming conditions. *Catalysts* **2019,** *9* (5), 473.